Measurement of D^0, D^+, D_s^+ and D^{*+} Production in Fixed Target 920 GeV Proton-Nucleus Collisions

HERA-B Collaboration

HERA-B Institutions

E-mail: x.xxx@xxx.xx

Abstract. The inclusive production cross sections of the charmed mesons D^0, D^+, D_s^+ and D^{*+} have been measured in interactions of 920 GeV protons on C, Ti, and W targets with the HERA-B detector at the HERA storage ring. Differential cross sections as a function of transverse momentum and x_F have been measured in the central rapidity region and for transverse momenta up to $p_T = 3.5$ GeV/c. The atomic number dependence and the leading to non-leading particle production asymmetries were measured as well.

Version 2.07, May 03, 2007

Summary of Comments on open-charm-paper-v3.dvi

This page contains no comments

1. Introduction

The cross sections for charm and beauty hadroproduction are of considerable theoretical interest [1]. Perturbative QCD is expected to work well for the large mass top quark production and less well for the lower mass b and c quarks [1, 2, 3]. At present, there exist several published results on measurements of charm production in proton-nucleus collisions [4]-[10]. They are mainly restricted to beam energies between 200 GeV and 800 GeV, and mostly have low statistics. Only one of the experiments also provided the measurement of the atomic number dependence. More and accurate data could help in determining the strong interaction parameters as well as guiding the calculation of non-perturbative effects. Another motivation comes from the recent observation that the ratio of open charm to charmonium cross section in pA reactions is essential for quark-gluon plasma searches [11]. The present work presents a new data point at 920 GeV proton beam energy.

Collisions of the 920 GeV HERA proton beam in C, Ti and W fixed targets have been measured with the HERA-B spectrometer. In previous papers we have reported on the $b\bar{b}$ [12], Υ [13], and charmonium [14] production cross sections, ~~whereas~~ the present work deals with production of open charm in the inclusive reactions $pA \to DX$. Here D represents a D^0, D^+, D_s^+ or D^{*+} detected through the following decay channels: $D^0 \to K^-\pi^+$, $D^+ \to K^-\pi^+\pi^+$, $D_s^+ \to \phi\pi^+ \to K^-K^+\pi^+$, and $D^{*+} \to D^0\pi^+ \to K^-\pi^+\pi^+$ and their charge conjugate.

The paper is organized as follows. We first briefly describe the apparatus, the data sample and the method of analysis. We then present the results, and finally make a comparison with other experiments and theoretical expectations.

2. The detector

HERA-B was a fixed target spectrometer (see Fig. 1) using the 920 GeV proton beam of the HERA e-p collider. Interactions occurred in two groups of 4 target wires separated by 4 cm [15]. The wires were located in the beam halo ~~in order not to disturb the other experiments measuring e-p collisions~~ and their distance to the beam core was automatically adjusted to maintain a constant interaction rate. Details of the various subdetectors have been published [16]-[22], so only a brief overview of the apparatus will be given here.

Tracks from proton interactions and decay vertices were measured with a vertex detector system (VDS) [16]. 64 silicon strip detectors with double-sided readout (50x70 mm^2, pitch of ~50 μm) were arranged in 8 stations between 7 cm and 200 cm downstream of the targets. The detectors were in Roman pots under vacuum and their ~~position~~ were adjusted within 10-15 *mm* from the beam center. With this system a vertex resolution of $\sigma_z \sim 500\mu$m along the beam direction and $\sigma_{x,y} \sim 50\mu$m in the transverse plane was achieved.

Particle momenta were measured with a tracking system and a dipole magnet of

Page: 2

Author: medinnis
Subject: Replacement Text
Date: 23.05.2007 15:50:02
while

Author: medinnis
Subject: Inserted Text
Date: 23.05.2007 15:50:20
s

Author: medinnis
Subject: Inserted Text
Date: 02.06.2007 23:02:38
with typical transverse dimensions betwen 50 and 500 microns

Author: medinnis
Subject: Replacement Text
Date: 02.06.2007 22:50:07
this is true but it's not the only reason. If the wire were directly in the beam it would burn retty quickly!

Author: medinnis
Subject: Inserted Text
Date: 02.06.2007 22:51:14
to

Author: medinnis
Subject: Replacement Text
Date: 02.06.2007 22:51:09
inner edges

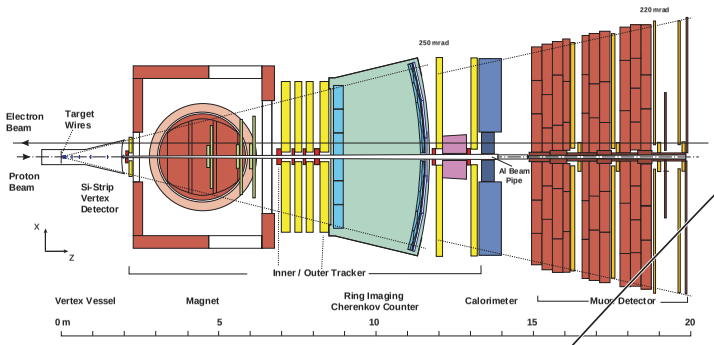

Figure 1. A top view of the HERA-B detector.

2.13 Tm field integral. The first tracking chamber was in front of the magnet, and remaining six chambers were behind the magnet between 7 m and 13 m downstream of the interaction region. The tracking chambers were located behind the magnet, up to 13 m downstream of the interaction region. Due to large differences in particle flux density, the tracking system was divided into a fine grained inner tracker (ITR - microstrip gas chambers with gas electron multipliers and typically 300 μm pitch) [17] and a coarse grained outer tracker (OTR - honeycomb drift cells with 5 mm and 10 mm wire pitches) [18]. The momentum resolution can be paramatrized as $\sigma_p/p = (1.61 + 0.0051pc/\mathrm{GeV})\%$ [19].

Particle identification was achieved with three subdetectors: the ring imaging Cherenkov counter (RICH), the electromagnetic calorimeter (ECAL) and the muon chambers (MUON). The RICH detector [20] is a large vessel containing about 100 m^3 of C_4F_{10} gas at NTP, which provided about 2 m of radiation path. The Cherenkov photons were focused and reflected by two sets of spherical and planar mirrors onto an upper and a lower photon detector. Each photon detector consisted of about 1100 multianode photomultiplier tubes. The pion efficiency was about 90% in the momentum range up to 70 GeV/c with the kaon misidentification probability below 10%, while the kaon efficiencies were above 85% for kaon momenta between 15 GeV/c and 45 GeV/c with the pion misidentification of $\sim$1%. For kaons below Cherenkov threshold of $\sim$10 GeV/c the misidentification of pions was kept below 10%.

The ECAL [21] was a sampling calorimeter of the "shashlik" type, with scintillator plates sandwiched between tungsten (inner region) or lead (outer region) absorbers and read out by optical fibers and PMTs. The readout granularity of inner and outer regions was also adapted to different particle rates in order to maintain acceptable occupancies. The MUON system [22], situated in the most downstream region, consisted of four large detector stations ~~which were~~ separated by iron absorbers. Each muon detector plane

Page: 3

Author: medinnis
Subject: Inserted Text
Date: 02.06.2007 22:53:01
where p is the particle momentum

Author: medinnis
Subject: Inserted Text
Date: 02.06.2007 22:55:30
slightly above pion threshold (x.x GeV) and

Author: medinnis
Subject: Cross-Out
Date: 02.06.2007 22:56:28

Table 1. Summary of the data statistics and the integrated luminosities of the present study.

Target	A	events [$\times 10^6$]	$\mathcal{L}$ [μb^{-1}]
C	12.01	89.3	375
Ti	47.88	24.7	31
W	183.84	67.6	36

had gas pixel chambers in the inner region and gas proportional tubes in the outer region.

For the present measurement, the analysis of data was based on the following components: the vertex detector (VDS), the OTR tracking system and the RICH counter.

3. Data analysis

The study was performed on data sets with only a single operational target wire made either of carbon, titanium or tungsten. Only runs with stable conditions and a minimum bias trigger with a total of 182 million interactions (table 1) were considered. The trigger required at least 20 hits in the RICH detector (compared to an average of 33 for a full ring from a $\beta = 1$ particle [20]) and was sensitive to $\epsilon_{\text{trigger}} > 97\%$ of the total inelastic cross section σ_{inel}. The integrated luminosity $\mathcal{L}$ was determined [23] from the number of inelastic interactions N_{inel} using the expression $\mathcal{L} = N_{\text{inel}}/(\epsilon_{\text{trigger}}\sigma_{\text{inel}})$. The data were recorded at a moderate interaction rate of about 1.5 MHz which corresponds to 0.17 interactions per filled bunch crossing. Therefore only about 10% of the events contain more than one interaction. The high data acquisition rate of about 1 kHz allowed to record the bulk of the data within two weeks.

At the HERA-B energy the charm production cross section is by more than two orders of magnitude smaller than the inelastic cross section. Taking into account also the relatively small branching ratios for the D meson decay modes into two or three charged particles in the final state, and the limited acceptance of the detector, one finds sizeable backgrounds if strict data selection criteria are not applied. Particle identification alone, for example, is not sufficient to extract signals. However, the large boost of the center-of-mass system of HERA-B ($\gamma = 22$), causing D mesons to decay several millimeters from the target, combined with a good vertex resolution ($\approx$0.5 mm) provides a possibility to distinguish D meson decay products from the particles originating at the primary interaction point. The data selection thus required a detached secondary vertex, formed by tracks not coming from the primary interaction point as well as the identification of kaons and pions. The analysis cuts are summarized in table 2, and discussed in some detail below.

This page contains no comments

3.1. Data selection

Since a detached vertex is required for the ground state D mesons, only events with at least one reconstructed primary vertex were selected. Primary vertices were determined from all track segments reconstructed in the VDS. Since the proton interaction point is inside the target wire, we replaced the measured primary vertex position in the coordinates transverse to the wire with the known target wire position.

For the tracks corresponding to the decay products of D mesons we demanded mild requirements on the number of hits in the vertex detector and the main tracking system, and on the track fit quality.

The following selection criteria based on the information from the RICH counter were used to identify the final state kaons and pions. While a rather strict cut on the kaon likelihood was required for the kaon candidates ($L_K > 0.5$ for the D^0 and D^+ selection, and $L_K > 0.33$ for D_s^+ candidates), for pions only a mild cut $L_e + L_\mu + L_\pi > 0.05$ was applied on the sum of RICH likelihoods for electrons, muons and pions. No particle identification requirement was imposed for pions from $D^{*+} \to D^0\pi^+$ decays, which we shall denote as slow pions, $\pi_{\rm slow}$.

The tracks were combined to D^0, D^+ and D_s^+ candidates. Candidates with an invariant mass in the interval of ± 0.5 GeV around the D meson nominal mass were considered in the further analysis. For the D_s^+ candidates, two additional cuts were applied. The invariant mass of the K^+K^- pairs was required to be in the interval of ± 10 MeV around the ϕ nominal mass; the absolute value of the cosine of the angle θ_ϕ between K^+ and π in the rest frame of the ϕ was restricted to the values above 0.5, exploiting the vector nature of the intermediate state ϕ. The D^{*+} candidates were combined from the D^0 candidates with invariant mass ± 75 MeV around the D^0 mass and the slow pions, after a vertex fit to D^0. For the D^{*+} candidates, an additional cut on the product of transverse momenta of the D^0 daughter tracks, $\zeta = p(D^0)p_{\rm T}(K)p_{\rm T}(\pi)$, was applied.

In addition to the cuts described above, we also restricted our analysis to the region of phase space with a high acceptance, $-0.15 < x_{\rm F} < 0.05$.

A common vertex for each track combination was fitted. Only combinations with a probability greater than 0.1% and with a secondary vertex displaced by more than 4 standard deviations downstream of the wire were accepted.

The D meson candidate was then associated with the primary vertex. In case of events with multiple reconstructed primary vertices, the one with the smallest impact parameter significance (i.e. the measured value divided by its estimated error given by the covariance matrix) with respect to the D meson candidate was chosen. To avoid a possible bias in the primary vertex position due to tracks from the D meson candidate, the primary vertex was refitted without the D daughter tracks.

The final set of criteria was based on the primary and secondary vertices. The main source of the background, combinations of particles emerging from the primary interaction point, could be reduced by the following three requirements: (1) the

Page: 5

Author: medinnis
Subject: Cross-Out
Date: 02.06.2007 23:04:35

Author: medinnis
Subject: Inserted Text
Date: 02.06.2007 23:05:28
form

Author: medinnis
Subject: Inserted Text
Date: 02.06.2007 23:11:03
I don't think you've done enough to tell the reader that you are also including charge conjugates. Maybe an appropriate footnote here would help or maybe above where you define D.

Author: medinnis
Subject: Replacement Text
Date: 02.06.2007 23:05:41
for

Author: medinnis
Subject: Inserted Text
Date: 02.06.2007 23:12:57
the

secondary vertex ~~is~~ detached, ~~(2) the tracks~~ forming the secondary vertex did not come from the primary interaction point and (3) the D meson candidate originated from the primary interaction point. To fulfill these criteria, we used the cuts on the following variables:

- $d(D)$ the distance significance of the secondary vertex to the primary interaction point given by the associated primary vertex,
- $b(\pi), b(K)$ the impact parameter significance of a pion or a kaon to the primary vertex (in case more than one primary vertex was found, the closest to the particle is chosen),
- $b(D)$ the impact parameter significance of a D meson candidate to the associated primary vertex.

We found that for the three body decays of D^+ and D_s^+, a more effective cut than the cuts on single impact parameter significances of daughter tracks is the cut on their product $b(K)b(\pi_1)b(\pi_2)$ and $b(K_1)b(K_2)b(\pi)$, respectively.

By studying the correlation between the cut on the product of impact parameter significances and the proper life time we found that we could improve the signal significance, if we apply also cuts of the form $\sqrt[3]{b(K)b(\pi_1)b(\pi_1)} > 4(t - t_0)$, for D^+, and $\sqrt{b(\phi)b(\pi)} > 0.75(t - t_0)$, for D_s^+. The proper life time t is in units of the D meson mean life time, the value of t_0 is determined in an optimization.

For each decay mode the optimal cuts were determined by maximizing the signal significance $S/\sqrt{S+B}$ with S being the number of signal events and B the number of background events in a $\pm 3\sigma$ window centered at the D meson nominal mass (signal window). The signal S was taken from Monte Carlo simulation and was scaled to the luminosity of real data by using an estimation for the production cross sections from fits to the published D meson cross sections [1]. For the D_s^+ the cross section was assumed to amount to 20% of the sum of the D^0 and D^+ cross sections [2].

In the case of ground state D mesons, the number of background events B was estimated from the real data side bands. For the D_s^+, the mass region of $\pm 50 MeV$ around the nominal mass of the D^+, where a contribution of the decay $D^+ \to \phi\pi^+$ is expected, was excluded from side bands. To reduce the sensitivity to statistical fluctuations, the side bands were chosen larger than the signal window. In the case of the D^{*+}, the wrong sign combinations from real data were used to estimate the background in the signal window. As is usually done for this decay, the signal was reconstructed in the mass difference $q = m(K, \pi, \pi_{\text{slow}}) - m(K, \pi) - m_\pi$ rather than in the invariant mass of the $K, \pi, \pi_{\text{slow}}$ combinations.

After applying the selection cuts, which are summarized in table 2, the remaining data were scanned for events with more than one D meson candidate. In case of the D^0, D^+ and D_s^+ channels, the candidate with the largest decay distance significance $d(D)$ was kept. For the D^{*+} analysis, first the candidates were selected where the intermediate D^0 had the largest decay distance significance. If more combinations used the same D^0

Page: 6

Author: medinnis
Subject: Replacement Text
Date: 02.06.2007 23:15:18
was

Author: medinnis
Subject: Inserted Text
Date: 02.06.2007 23:20:03
to be

Table 2. Analysis cuts

$D^0 \to K^-\pi^+$	$D^+ \to K^-\pi^+\pi^+$
not optimized	
$L_K(K) > 0.5$	$L_K(K) > 0.5$
$L_e(\pi) + L_\mu(\pi) + L_\pi(\pi) > 0.05$	$L_e(\pi) + L_\mu(\pi) + L_\pi(\pi) > 0.05$
optimized	
$d(D^0) > 6.1$	$b(D^+) < 2.6$
$b(D^0) < 2.4$	$b(K)b(\pi_1)b(\pi_2) > 106$
$b(K) > 3.4$	$\sqrt[3]{b(K)b(\pi_1)b(\pi_2)} > 4(t - t_0),\ t_0 = 2.48$
$b(\pi) > 3.7$	

$D_s^+ \to \phi\pi^+ \to K^-K^+\pi^+$	$D^{*+} \to D^0\pi^+ \to K^-\pi^+\pi^+$
not optimized	
$L_K(K) > 0.33$	$L_K(K) > 0.5$
$L_e(\pi) + L_\mu(\pi) + L_\pi(\pi) > 0.05$	$L_e(\pi) + L_\mu(\pi) + L_\pi(\pi) > 0.05$
$\lvert m(K^+K^-) - m(\phi)\rvert < 10MeV$	$\lvert m(K\pi) - m(D^0)\rvert < 75MeV$
$\lvert\cos(\theta_\phi)\rvert > 0.5$	
optimized	
$d(D_s^+) > 5.3$	$b(D^0) < 2.4$
$b(D_s^+) < 2.11$	$b(K) > 2.1$
$b(K^-)b(K^+)b(\pi) > 28.7$	$b(\pi) > 1.7$
$\sqrt{b(\phi)b(\pi)} > 0.75(t - t_0),\ t_0 = 1.0$	$\zeta(D^0) > 17.7(GeV/c)^3$

candidate in combination with a different $\pi_{\rm slow}$, the candidate with the highest vertex probability was kept.

3.2. Signal yields

The invariant mass distributions for D meson candidates after applying the selection criteria discussed above are shown in figure 2, ~~figure~~ 3 and ~~figure~~ 4.

To extract the signal yield, the histograms were fitted by a Gaussian function for the signal, while the background description depended on the type of the D meson. For the D^+ and D_s^+, the background was fitted by an exponential function. The background in the D^0 reconstruction is more complicated and consists of a combinatorial part, fitted by an exponential and a background from partially reconstructed charm decays. This background is noticeable for the mass range below the D^0 peak. We took the shape of the charm background from the Monte Carlo simulation of $c\bar{c}$ events, ~~after applying the analysis cuts~~.

In the D_s^+ invariant mass distribution also the Cabibbo suppressed decay of $D^+ \to \phi\pi^+$ is seen (the peak to the left from the D_s^+ peak). We included this peak

Page: 7

Author: medinnis
Subject: Cross-Out
Date: 02.06.2007 23:22:47

Author: medinnis
Subject: Cross-Out
Date: 02.06.2007 23:22:41

Author: medinnis
Subject: Inserted Text
Date: 02.06.2007 23:22:33
s

Author: medinnis
Subject: Replacement Text
Date: 02.06.2007 23:24:30
to which analysis cuts had been applied.

Table 3. Number of reconstructed D mesons.

sample	D^0	D^+	D_s^+	D^{*+}
total	174.8±16.8	130.5±14.7	11.4±4.0	61.3±13.0
particle	75.9±10.9	54.5± 9.3	4.9±2.6	21.0± 6.6
anti-particle	99.0±11.9	75.8±10.5	6.7±2.8	40.6± 8.3
C	66.1± 9.6	43.1± 7.7	4.2±2.2	26.6± 6.4
W	92.3±11.7	72.4±10.6	6.7±3.0	24.8± 7.5
Ti	17.4± 5.7	14.9± 5.0	0.4±1.0	9.6± 4.0

in the fit function as an additional Gaussian of the same width as the signal Gaussian, with normalization as an additional free parameter, while its mean was fixed to the value extracted from the $D^+ \to K^-\pi^+\pi^+$ invariant mass distribution.

The background in the D^{*+} reconstruction was parameterized as $a(q^{1/2} + bq^{3/2})$ with a and b as free parameters.

The fitted peak positions are within one standard deviation from the corresponding PDG values [24], with the exception of D_s^+, which deviates by two standard deviations. The widths of the signal peaks are by about 30% larger than the corresponding Monte Carlo values.

The numbers of reconstructed D mesons are summarized in table 3. In total, we reconstructed 175 D^0, 131 D^+, 11 D_s^+ and 61 D^{*+} decays. The signals in subsamples (particle, anti-particle, individual target material) were fitted by fixing the mean and σ of the signal Gaussian function to the values obtained from the fit to the full sample.

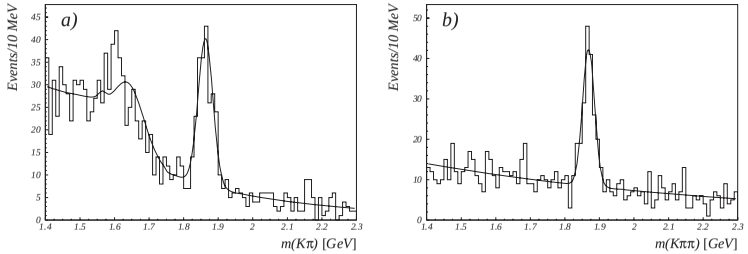

Figure 2. Invariant mass distributions for $K^-\pi^+$ (a) and $K^-\pi^+\pi^+$ (b) combinations.

To check the signal consistency, we measured the D meson proper time distributions. We checked that the acceptance corrected distributions are exponential and that the fitted lifetimes are in agreement with the PDG values. We used a simultaneous likelihood fit of events in the signal window and in the side bands. The results for all three mesons, $c\tau = (302 \pm 33)$ μm for D^+, (120 ± 13) μm for D^0, and (165 ± 52) μm for D_s^+, are in good agreement with the PDG values.

Page: 8

Author: medinnis
Subject: Replacement Text
Date: 02.06.2007 23:26:42
of

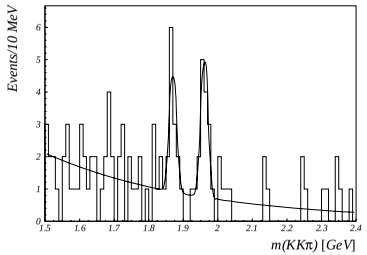

Figure 3. Invariant mass distributions for $\phi\pi^+ \to (K^-K^+)\pi^+$ combinations. Besides the D_s^+ peak at 1.96 GeV also the D^+ peak at 1.87 GeV is seen, corresponding to the Cabibbo suppressed decay $D^+ \to \phi\pi^+$.

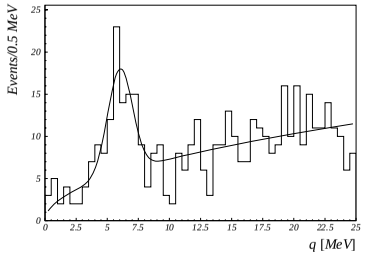

Figure 4. Invariant mass difference q for $K^-\pi^+\pi^+$ and $K^-\pi^+$ combinations.

As a further consistency check of the D_s^+ and D^{*+} signals, we checked the intermediate states ϕ and D^0, respectively. Intermediate states should be visible in the corresponding invariant mass distributions, when the signal region in the initial state invariant mass distribution is selected, and the fit to the intermediate state invariant mass distribution should give the number of events consistent with the number in the initial state peak. The yields extracted in this way are in good agreement with the values given in table 3. We further checked the distribution of the cosine of the angle between K^+ and π in the rest frame of the ϕ; the resulting distribution was consistent with the expectation given by the vector nature of the intermediate state ϕ. The consistency of the $D^+ \to \phi\pi^+$ signal in figure 3 was tested by estimating the number of reconstructed decays from our measured D^+ cross section in the $D^+ \to K^-\pi^+\pi^+$ decay channel. The fitted number of events, 9.8±3.8, is in reasonable agreement with the estimated number (4.2±1.2).

This page contains no comments

4. Efficiency determination

A Monte Carlo simulation is used to determine the signal reconstruction efficiencies. The Monte Carlo samples for $pA \to DX$ are generated in two steps. First, a $c\bar{c}$ pair is generated with Pythia 5.7 [26] such that a particular D meson is always produced. The generated events are reweighted to make the resulting cross sections conform to the parameterizations

$$\frac{d\sigma}{dp_{\mathrm{T}}^2} \propto [1 + (\frac{\sqrt{\pi}\ \Gamma(\beta - \frac{3}{2})\ p_{\mathrm{T}}}{2\ \Gamma(\beta - 1)\ \langle p_{\mathrm{T}} \rangle})^2]^{-\beta} \tag{1}$$

and

$$\frac{d\sigma}{dx_{\mathrm{F}}} = \begin{cases} Ae^{-\frac{x_{\mathrm{F}}^2}{2\sigma_g^2}} & , \quad |x_{\mathrm{F}}| < x_{\mathrm{b}} \\ A'(1 - |x_{\mathrm{F}}|)^n & , \quad |x_{\mathrm{F}}| \geq x_{\mathrm{b}} \end{cases} \tag{2}$$

with $\sigma_g = \sqrt{\frac{x_{\mathrm{b}}(1-x_{\mathrm{b}})}{n}}$ and $\ln \frac{A}{A'} = n(\frac{x_{\mathrm{b}}}{2(1-x_{\mathrm{b}})} + \ln(1 - x_{\mathrm{b}}))$ [10]. The average transverse momentum of $\langle p_{\mathrm{T}} \rangle = 1.04 \pm 0.04$ GeV/c and the value of the exponent $\beta = 7.0 \pm 4.3$ are taken from the present analysis (Sec. 5.2). We took $n = 7.7 \pm 1.4$ from the average of E653 and E743 [7, 6], and $x_{\mathrm{b}} = 0.062 \pm 0.013$ as measured by the E791 experiment [10]. The influence of the parameter uncertainties and other possible parametrisations of expression (2) is taken into account as a systematic error. After the generation of the D mesons, the remaining energy is given as input to the Fritiof 7.02 [27] program package which generates the underlying event taking into account further interactions inside the nucleus.

The detector response is simulated with the Geant 3.21 package [25]. Realistic detector efficiencies, readout noise and dead channels are taken into account. The simulated events are processed by the same reconstruction codes as the data.

5. Results

5.1. Total cross sections

The visible cross section per nucleus, i.e. the cross section measured in our visible range of $-0.15 < x_{\mathrm{F}} < 0.05$, is given by

$$\Delta\sigma_{\mathrm{pA}} = \frac{N_i}{Br \cdot \epsilon_i \cdot \mathcal{L}_i} \tag{3}$$

where N_i is the number of reconstructed D mesons, ϵ_i and $\mathcal{L}_i$ are the efficiency and integrated luminosity for a particular target and Br the branching ratio for a specific decay channel [24]. The cross section for D meson production on a nuclear target of atomic number A is parameterized as

$$\sigma_{\mathrm{pA}} = \sigma_{\mathrm{pN}} \cdot A^{\alpha} \tag{4}$$

To combine data recorded with different target materials, the production cross sections per nucleon $\Delta\sigma_{\mathrm{pN}}$ was extracted in the following way. From equations (3) and (4) we

This page contains no comments

Table 4. Summary of systematic uncertainties of reconstruction efficiency.

Source	D^0	D^+	D_s^+	D^{*+}
Monte Carlo statistics	1.2%	1.3%	3.7%	1.1%
Track reconstruction	3.0%	4.5%	4.5%	4.5%
Particle identification	4.0%	6.0%	6.0%	4.0%
Analysis cuts	6.0%	6.0%	6.0%	6.0%
Re-weighting	2.9%	3.6%	7.7%	4.6%
Total	8.4%	10.3%	12.9%	9.7%

derive for the D meson yield of the target i

$$N_i = Br \cdot \epsilon_i \cdot \mathcal{L}_i \cdot \Delta\sigma_{\mathrm{pN}} \cdot A_i^{\alpha} \tag{5}$$

By summing (5) over all targets and solving it for the production cross section we get

$$\Delta\sigma_{\mathrm{pN}} = \frac{N}{Br \cdot \sum_i \epsilon_i \mathcal{L}_i A_i^{\alpha}}, \tag{6}$$

where $N = \sum_i N_i$ is the measured D meson yield of the total data sample. The sum in the denominator of (6) can be rewritten by introducing the average efficiency ϵ, defined by the weighted sum:

$$\epsilon = \sum_i p_i \epsilon_i \quad , \qquad p_i = \frac{A_i^{\alpha}\mathcal{L}_i}{\sum_k A_k^{\alpha}\mathcal{L}_k} \tag{7}$$

Then the expression (6) reads

$$\Delta\sigma_{\mathrm{pN}} = \frac{N}{Br \cdot \epsilon \cdot \sum_i \mathcal{L}_i A_i^{\alpha}} \tag{8}$$

Since there is no experimental indication for nuclear effects in open charm production, we assumed a linear A dependence of the production cross sections and set $\alpha = 1$ in (7) and (8).

The total systematic uncertainties are, according to (8), composed of contributions from event counting, branching fractions, integrated luminosity and reconstruction efficiency. Furthermore, the uncertainty of the reconstruction efficiency can be divided into contributions from Monte Carlo statistics, track reconstruction efficiency, particle identification efficiency, analysis cuts and the contribution from the reweighting of kinematical distributions. The individual contributions are summarized in table 4 and table 5. The uncertainty due to analysis cuts was determined in two ways, by varying the cut values and by performing an independent analysis.

The resulting cross sections in the visible range, $\Delta\sigma_{\mathrm{pN}}$ and $\Delta\sigma_{\mathrm{pA}}$, are summarized in table 6, table 7, and table 8. In order to extrapolate the measurements to the full phase space,

$$\sigma_{\mathrm{pN}} = \frac{\Delta\sigma_{\mathrm{pN}}}{f_{\mathrm{vis}}}, \tag{9}$$

we determined the fraction f_{vis} of D mesons in the visible range defined by $-0.15 < x_{\mathrm{F}} < 0.05$. With the measured value of the exponent $n = 7.7 \pm 1.4$ as measured by

This page contains no comments

Table 5. Summary of systematic uncertainties of visible cross sections

Source	D^0	D^+	D_s^+	D^{*+}
Event counting	3.4%	2.6%	6.0%	9.7%
Branching fractions	1.8%	3.6%	13.0%	1.9%
Luminosity	3.4%	3.4%	3.4%	3.4%
Efficiency	8.4%	10.3%	12.9%	9.7%
Total	10%	12%	20%	14%

the E653 and E743 experiments [7, 6], we calculated $f_{\rm vis}$ by using the expression (2). The values corresponding to the choice $x_{\rm b} = 0.062$ and $x_{\rm b} = 0$ are 0.542±0.048 and 0.558±0.051, respectively. The difference is small compared to the uncertainty due to the error of parameter n. For the extrapolation we used the average of both numbers, $f_{\rm vis} = 0.55 \pm 0.05$. The resulting cross sections extrapolated to the full phase space are listed in table 6.

Figure 5 shows the comparisons of the measured cross sections with other experimental studies. To compare the data points at different center-of-mass energies, the expression

$$\sigma(\sqrt{s}) = p_0 \left(1 - \frac{p_1}{\sqrt{s}^{p_3}}\right)^{p_2} \tag{10}$$

given in [1] was fitted to the data. This equation and the way of fitting for the different PDFs was taken from [1]. In the fits to the data points only the normalization was left free, and our measurement was included in the fit. Our results provide the most accurate measurement at high energies, and are consistent with previous studies.

Table 6. Cross sections in the visible range ($-0.15 < x_{\rm F} < 0.05$) and extrapolated to the full phase space. In the second column, the systematic error due to the extrapolation uncertainty is quoted separately.

	$\Delta\sigma_{\rm pN}[\mu b]$ (visible range)	$\sigma_{\rm pN}[\mu b]$ (full $x_{\rm F}$ range)
D^0	26.8±2.6±2.7	48.7±4.7±4.9±4.4
D^+	11.1±1.2±1.3	20.2±2.2±2.4±1.8
D_s^+	10.2±3.5±2.0	18.5±6.4±3.7±1.7
D^{*+}	11.9±2.6±1.7	21.6±4.7±3.0±2.0

Table 7. Cross sections for particle and anti-particle production in the visible range ($-0.15 < x_{\rm F} < 0.05$).

	$\Delta\sigma_{\rm pN}[\mu b]$			
	D^0	D^+	D_s^+	D^{*+}
particles	12.0±1.7±1.2	4.8±0.8±0.6	4.1±2.3±0.8	4.5±1.4±0.6
anti-particles	14.8±1.7±1.5	6.3±0.9±0.8	6.3±2.6±1.3	7.2±1.5±1.0

Page: 12

Author: medinnis
Subject: Inserted Text
Date: 05.06.2007 11:35:24
I guess the other parameters were fixed to the numbers given in 1?

Table 8. Visible cross sections per nucleus. Numbers in ~~parenthesis~~ of the last row are for the subsamples of D^{*+} with D^0 daughter not common to the D^0 samples of the first column.

	$\Delta\sigma_{pA}$ [mb]		
data sample	C	Ti	W
D^0	0.36± 0.05± 0.04	1.01± 0.33± 0.10	4.91± 0.62± 0.54
D^+	0.12± 0.02± 0.02	0.48± 0.16± 0.06	2.17± 0.32± 0.28
D_s	0.12± 0.07± 0.02	0.15± 0.35± 0.03	2.18± 0.99± 0.46
D^{*+}	0.17± 0.05± 0.03	0.71± 0.30± 0.10	1.71± 0.51± 0.26
	(0.21± 0.06± 0.03)	(0.95± 0.50± 0.14)	(2.11± 0.84± 0.34)

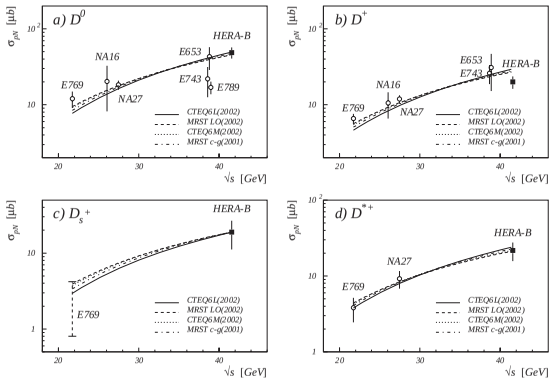

Figure 5. Measured cross section, comparison of the results with previous experiments. In figure a) the result of E789 was excluded from the fit.

Note that to account for a general value of α, $\alpha \neq 1$, the cross section can be parametrized as $\sigma_{pN}(\alpha) = \sigma_{pN}(\alpha = 1) + d\sigma_{pN}/d\alpha \cdot (\alpha - 1)$. The corresponding coefficient $d\sigma_{pN}/d\alpha = -4.1\sigma_{pN}$ is determined from (6) and data in table 1.

The sum of the D-meson cross sections per nucleon $\sigma(D^0) + \sigma(D^+) + \sigma(D_s^+) = (87.4 \pm 8.2 \pm 12.6)\mu$b accounts for $(89.1 \pm 4.1)\%$ of the charm cross section [24]. The resulting charm cross section per nucleon is $\sigma(c\bar{c}) = (49.1 \pm 4.6 \pm 7.4)\mu$b. Due to correlations, the systematic error is slightly larger than the value which one would get by adding in quadrature the individual contributions.

Page: 13

Author: medinnis
Subject: Replacement Text
Date: 05.06.2007 11:28:40
in

Author: medinnis
Subject: Replacement Text
Date: 05.06.2007 11:28:26
parentheses

Author: medinnis
Subject: Inserted Text
Date: 05.06.2007 11:28:57
s

Author: medinnis
Subject: Inserted Text
Date: 05.06.2007 11:32:15
I could easily have missed it but this point deserves some discussion in the text -- I'm not sure what it means.

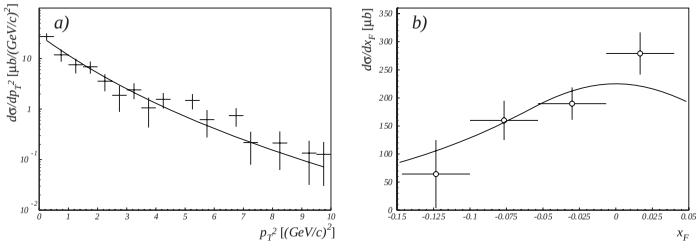

Figure 6. Differential visible cross sections ($-0.15 < x_F < 0.05$) for D^0 and D^+ production: (a) $d\sigma/dp_T^2$, with the fit of expression (1), and (b) $d\sigma/dx_F$ with a fit of function (2) with a free parameter n and a fixed boundary parameter $x_b = 0.062$.

5.2. Differential cross sections

The differential cross sections $d\sigma/dp_T^2$ and $d\sigma/dx_F$ were determined from production yields in bins of p_T^2 and x_F by using the expression (8). The yield in each individual bin was determined by subtracting from the number of events in the D meson signal window the number of background events as determined from the side bands. The resulting differential cross sections for the production of D^0 and D^+ mesons are shown in figure 6.

For the transverse momentum distribution, several parametrisations have been found in the literature. We have used the parametrisation given in expression (1), and extracted the values of parameters $\langle p_T \rangle$ and β from a fit to the data.

The distribution of background events $N_{bgr}(p_T^2)$ was assumed to be the same in shape and normalization for the signal window and side bands. Several parameterizations were fitted first to the distributions of the events from side bands. As many of them fit well, we chose the one among those with two free parameters which gave the smallest χ^2/ndf, $e^{A+Bp_T^2}$ for D^0 and D^+, and the same parametrisation multiplied with the efficiency in p_T^2, $e^{A+Bp_T^2}\epsilon(p_T^2)$, for D^{*+}.

The parameters were determined by a simultaneous maximum likelihood fit of events in the signal window and in the side bands. We simultaneously fitted the D^0, D^+ and D^{*+} data samples, where in the D^{*+} case only a subsample was considered with the D^0 daughters not common to the D^0 sample. The resulting fit parameters are $\langle p_T \rangle = (1.04 \pm 0.04)$GeV/$c$ and $\beta = 7.0 \pm 4.3$, with $\chi^2/ndf = 0.82$. The measured $\langle p_T \rangle$ is significantly larger (by 3.3σ) than the value extracted from the Pythia Monte Carlo data (0.90 GeV/c), while β is within one standard deviation equal to the value extracted from the Monte Carlo data ($\beta = 4.80$). We repeated the fit with the fixed value of $\beta = 6$, the same value that was also used on our study of J/ψ production [14]. In this case we get the same value, $\langle p_T \rangle = (1.04 \pm 0.04)$GeV/$c$, for $\langle p_T \rangle$, with $\chi^2/ndf = 0.81$.

Page: 14

Author: medinnis
Subject: Replacement Text
Date: 05.06.2007 11:42:34
in

The x_F distribution is usually parameterized with a power-law function:

$$\frac{d\sigma}{dx_F} \propto (1 - |x_F|)^n \tag{11}$$

When compared to the predictions from the next-to-leading order QCD calculations this function does not reproduce well the central region [3]. The experimental observation made by E791 [10] in 500 GeV π-A collisions using a high statistics sample of 80k reconstructed D^0 mesons also shows a similar discrepancy. They fitted their data with a function given in (2) (to account for the asymmetry in π-A collisions they used an additional offset parameter in their original parametrisation), an extension of (11), which uses a power-law function in the tail region and a Gaussian in the central region.

In our analysis of the measured differential cross section $d\sigma/dx_F$ (figure 6(b)), the boundary parameter x_b was fixed to the value $x_b = 0.062$ as measured by E791 [10], because our range of $-0.15 < x_F < 0.05$ is too small to be sensitive to this parameter. To extract the exponent n, we ~~fitted~~ simultaneously the D^0 and D^+ data samples with a likelihood fit to the events in the signal windows and sidebands. While the fitted value of the exponent $n = 7.5 \pm 3.2$ agrees with the results of E653 [7] and E743 [6], the error in our study is much larger.

5.3. Cross section ratios

The measured cross section ratios are summarized in table 9. The systematic errors mainly come from analysis cuts, event counting, branching fraction uncertainties and reweighting, while the error in luminosity cancels. The value for the ratio $\sigma(D^+)/\sigma(D^0) = 0.41 \pm 0.06 \pm 0.04$ is the most accurate measurement of this ratio in pA reactions. It is in good agreement with the latest predictions of Pythia [1] and with the combined results from hadroproduction [1] as well as from e^+e^- experiments [24]. A comparison with results from other experimental studies is presented in figure 7. The ratio $\sigma(D^{*+})/\sigma(D^0) = 0.44 \pm 0.11 \pm 0.05$ is again the most precise measurement of this ratio in pA reactions, and in good agreement with the results of E769 and NA27. Both ratios are also in agreement with the predictions of a simple isospin model [2]. The vector to scalar meson production ratio can be calculated in different ways ([1] and references therein), if isospin invariance is assumed. From the ratio $R_1 = \sigma(D^+)/\sigma(D^0)$ we get $P_V = (1 - R_1)/(1 + R_1)/Br(D^{*+} \to D^0\pi^+) = 0.61 \pm 0.09 \pm 0.06$, and from $R_2 = \sigma(D^{*+})/\sigma(D^+)$ the value $P_V = R_2/(1+Br(D^{*+} \to D^0\pi^+)\cdot R_2) = 0.62 \pm 0.09 \pm 0.05$. The results are in perfect agreement with the world average value $P_V = 0.59 \pm 0.01$ [1].

Our result for the ratio $\sigma(D_s^+)/(\sigma(D^0) + \sigma(D^+)) = 0.27 \pm 0.09 \pm 0.05$ is the first measurement of this quantity in pA reactions. It is in agreement within 1.6 standard deviations with the world average value of 0.13 ± 0.04 of measurements in e^+e^- collisions [24].

Page: 15

Author: medinnis
Subject: Cross-Out
Date: 05.06.2007 11:44:13

Author: medinnis
Subject: Inserted Text
Date: 05.06.2007 11:44:19
fitted

Table 9. Cross section ratios

D^+/D^0	D^{*+}/D^0	$D_s^+/(D^+ + D^0)$	D^{*+}/D^+
0.41±0.06±0.04	0.44±0.11±0.05	0.27±0.09±0.05	1.07±0.26±0.14

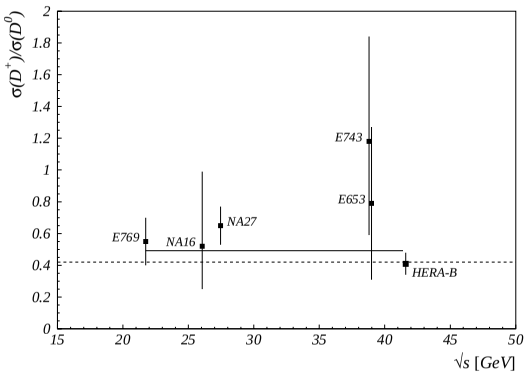

Figure 7. Cross section ratio $R = \sigma(D^+)/\sigma(D^0)$, comparison with previous experiments. The dotted line at $R = 0.42$ shows the prediction of the isospin model with $P_V = 0.6$ [1].

5.4. Leading to non leading particle asymmetries

The leading particle is defined as the one which has a light quark in common with the beam particle. Thus the leading particles are anti-D mesons $\bar{D}^0$, D^- and D^{*-}. The leading to non-leading particle asymmetry is defined as $(\sigma_{LP} - \sigma_{nonLP})/(\sigma_{LP} + \sigma_{nonLP})$. The measured values of the asymmetry in the visible range, $-0.15 < x_F < 0.05$, are 0.10±0.09±0.05, 0.14±0.11±0.06 and 0.23±0.17±0.06 for the D^0, D^+ and D^{*+} mesons, where the first error is statistical and the second systematic. The latter is dominated by the uncertainty of analysis cuts and the kinematical reweighting in respect to possible differences between leading and non-leading particles. Our measurements are in good agreement with the existing measurements of this asymmetry for the D^0 and D^+ mesons [8], as well as with Pythia predictions, 0.24, 0.22, and 0.23 for the D^0, D^+, and D^{*+} mesons, respectively. The weighted average of the D^0, D^+ and D^{*+} asymmetries is 0.13±0.06±0.01, i.e. two standard deviations above zero and within 1.5 standard deviations of the Pythia prediction.

This page contains no comments

Table 10. Atomic number dependency parameter α and a weighted average for the four D mesons. For the weighted average the value in parenthesis of the fifth row were used, corresponding to the subsample of D^{*+} with D^0 daughter not common with the D^0 sample.

Particle	α
D^0	0.969±0.057±0.026
D^+	1.051±0.082±0.028
D_s^+	1.190±0.402±0.046
D^{*+}	0.832±0.138±0.022
	(0.847±0.185±0.022)
Average	0.994±0.044±0.025

5.5. Atomic mass number dependence

From the measured D meson production on three different target materials (table 8), the exponent α of the relation (4) can be determined. The results of simultaneous maximum likelihood fits to the invariant mass distributions of individual material data samples for each D meson are summarized in table 10. The systematic error comes from two contributions, uncertainty in the luminosity per wire material (about 2.5%) and Monte Carlo statistics (about 1%). The observed value, $\alpha = 0.99 \pm 0.04 \pm 0.03$, is compatible with a linear dependence of cross sections ($\alpha = 1$). Note that for the weighted average of the parameter α over all four D meson samples we took only those D^{*+} events, for which the D^0 daughter particle was not reconstructed in the D^0 sample. Our result is in agreement with the result of E789 [9], $\alpha = 1.02 \pm 0.03 \pm 0.02$.

6. Summary

With the HERA-B detector we measured the total and single differential cross sections σ, $d\sigma/dp_{\mathrm{T}}^2$ and $d\sigma/dx_{\mathrm{F}}$, the atomic number dependence of the cross sections and the leading to non-leading particle asymmetries for the production of D^0, D^+, D_s^+ and D^{*+} mesons in pA collisions at the proton energy of 920 GeV.

Extrapolated to the full phase space the total cross sections per nucleon (in μb) are: 48.7±4.7±6.6, 20.2±2.2±3.0, 18.5±6.4±4.1 and 21.6±4.7±3.6 for the D^0, D^+, D_s^+ and D^{*+}, respectively and in the visible x_{F} range $-0.15 < x_{\mathrm{F}} < 0.05$: 26.8±2.6±2.7, 11.1±1.2±1.3, 10.2±3.5±2.0 and 11.9±2.6±1.7 for the D^0, D^+, D_s^+ and D^{*+} respectively. The cross section per nucleon for $c\bar{c}$ production is $\sigma(c\bar{c}) = (49.1 \pm 4.6 \pm 7.4)\mu$b.

We also measured the cross section ratios $\sigma(D^+)/\sigma(D^0) = 0.41 \pm 0.06 \pm 0.04$ and $\sigma(D^{*+})/\sigma(D^0) = 0.44 \pm 0.11 \pm 0.05$, as well as the vector to scalar meson production ratio in two ways, $P_{\mathrm{V}} = 0.61 \pm 0.09 \pm 0.06$, and $P_{\mathrm{V}} = 0.62 \pm 0.09 \pm 0.05$. Our result for the ratio $\sigma(D_s^+)/(\sigma(D^0)+\sigma(D^+))$= 0.27±0.09±0.05 is the first measurement of this quantity in pA reactions, and is in agreement with measurements in e^+e^- collisions.

This page contains no comments

From the measured atomic number dependence of the production cross section, the parameter $\alpha = 0.99 \pm 0.04 \pm 0.03$ was extracted. This value is in good agreement with the assumption of a linear dependence of cross sections, α=1. The measured leading to non-leading particle asymmetries in the x_F range $-0.15 < x_F < 0.05$ are in good agreement with the predictions derived from Pythia.

While the results of our studies are in good agreement with previous measurements, they provide in most cases the most accurate measurements in pA interactions.

References

[1] Lourenco C and Woehri H 2006 *Phys. Rept.* **433** 127
[2] Frixione S, Mangano M L, Nason P and Ridolfi G, 1998 *Adv.Ser.Direct High energy Phys.* **15** 609
[3] Nason P, Dawson, S and Ellis R K 1989 *Nucl. Phys.* **B327** 49
[4] Aguilar-Benitez M *et al* (LEBC-EHS Collaboration) 1984 *Phys. Lett.* B **135** 237
[5] Aguilar-Benitez M *et al* (LEBC-EHS Collaboration) 1988 *Z. Phys.* C **40**, 321
[6] Ammar R *et al* (E743 Collaboration) 1988 *Phys. Rev. Lett.* **61**, 2185
[7] Kodama K *et al* (E653 Collaboration) 1991 *Phys. Lett.* B **263**, 573
[8] Alves G A *et al* (E769 Collaboration) 1996 *Phys. Rev. Lett.* **77**, 2388 (Erratum-ibid. 1998 **81** 1537)
[9] Leitch M J *et al* (E789 Collaboration) 1994 *Phys. Rev. Lett.* **72** 2542
[10] Aitala E M *et al* (E791 Collaboration) 1999 *Phys. Lett.* B **462** 225
[11] Cacciari M, Nason P, Vogt R 2005 *Phys. Rev. Lett.* **95** 122001
[12] Abt I (HERA-B Collaboration) *et al* 2006 *Phys. Rev.* D **73** 052005
[13] Abt I (HERA-B Collaboration) *et al* 2006 *Phys. Lett.* B **638** 13
[14] Abt I (HERA-B Collaboration) *et al* 2006 *Phys. Lett.* B **638** 407
[15] Ehret K *et al* 2000 *Nucl. Instrum. Methods* A **446** 190
[16] Bauer C *et al* 2003 *Nucl. Instrum. Methods* A **501** 39
[17] Gradl W *et al* 2001 *Nucl. Instrum. Methods* A **461** 80
[18] Albrecht H *et al* 2005 *Nucl. Instrum. Methods* A **541** 610
[19] Albrecht H *et al* 2007 *Nucl. Instrum. Methods* A **576** 313
[20] Ariño I *et al* 2004 *Nucl. Instrum. Methods* A **516** 445
[21] Avoni G *et al* 2001 *Nucl. Instrum. Methods* A **461** 332
[22] Eiges V *et al* 2001 *Nucl. Instrum. Methods* A **461** 104
[23] Bruschi M 2005 "Luminosity determination at HERA-B" HERA-B Note 05-11
[24] Yao W M *et al* (Particle Data Group) 2006 *J. Phys. G: Nucl. Part. Phys.* **33** 1.
[25] Brun R *et al* 1987 *GEANT3* (Internal Report CERN-DD/EE/84-1, CERN).
[26] Sjostrand T 1994 Comp. Phys. Commun. **82** 74
[27] Pi H 1992 Comp. Phys. Commun. **71** 173

Page: 18

Author: medinnis
Subject: Inserted Text
Date: 05.06.2007 12:01:34
We can now reference the hep archive number: arXiv: 0706.0131